

Endohedral ^1H NMR Chemical Shifts of H_2 -, H_2O - and NH_3 -Encapsulated Fullerene Compounds: Accurate Calculation and Prediction

Guan-Wu Wang,^{*,[a]} Ping Wu,^[a] and Zhi-Guo Tian^[a]

Keywords: Fullerenes / Density functional calculations / Semiempirical calculations / NMR spectroscopy

The endohedral ^1H NMR chemical shifts of various known H_2 -, H_2O - and NH_3 -encapsulated fullerene compounds have been calculated at the GIAO-B3LYP/3-21G and GIAO-HF/3-21G levels of theory with AM1- and PM3-optimized structures. The corrected ^1H NMR chemical shifts were calculated from the correlation equation derived from linear regression fitting between calculated and experimental ^1H NMR chemical shifts in each case. Comparisons of the regression coefficients, standard deviations, and maximum and mean errors of the corrected chemical shifts obtained by the four methods employed showed that the GIAO-B3LYP/3-21G//PM3 method is the best for calculating the endohedral ^1H NMR chemical shifts of endofullerenes. The endohedral ^1H NMR

chemical shifts of any H_2 -, H_2O - or NH_3 -encapsulated fullerene compound can be predicted by the correlation equation derived by using the GIAO-B3LYP/3-21G//PM3 method. The shift tendency of endohedral ^1H NMR chemical shifts are discussed and compared with that of endohedral ^3He NMR chemical shifts. The encapsulated H_2 , H_2O or NH_3 molecule can be employed as a sensitive NMR probe to investigate the ring currents of fullerene cages and to follow the chemical reactions of endofullerenes at the exterior of the fullerene cage.

(© Wiley-VCH Verlag GmbH & Co. KGaA, 69451 Weinheim, Germany, 2009)

Introduction

Endohedral fullerene are expected to have widespread applications in materials science and technology.^[1] In the early days, endohedral fullerenes could only be accessed by physical processes, such as co-vaporization of carbon and metal atoms^[2] and high-pressure/high-temperature treatment with noble gases.^[3] However, chemical modification/molecular surgery has recently emerged as a new route to producing endohedral fullerenes. A number of open-cage fullerene derivatives, most of which are C_{60} derivatives, have been reported to possess the ability to encapsulate He ,^[4] H_2 ,^[4a,4c,5,6] H_2O ,^[7] CO ^[8] or NH_3 .^[9] The milestone synthesis of $\text{H}_2@\text{C}_{60}$ was achieved by Komatsu et al. who closed the thirteen-membered ring orifice of a hydrogen-encapsulated open-cage fullerene by using a four-step organic reaction sequence.^[6] The characterization of these derivatives is important due to the increasing interest in endofullerenes. As an important tool for identifying these molecules, NMR spectroscopic analysis of encapsulated atoms or molecules such as He , H_2 , H_2O or NH_3 has an unprecedented advantage.

In 1994, the endohedral chemical shifts of fullerenes were first calculated by Haddon and Pasquarello by the semiem-

pirical London method. They calculated ^3He NMR chemical shifts of -10.1 ppm for $^3\text{He}@\text{C}_{60}$ and -16.8 ppm for $^3\text{He}@\text{C}_{70}$,^[10] which clearly deviate from the experimental values of -6.3 and -28.8 ppm.^[3b] With the development of computational methodologies and sources, improved theoretical levels such as GIAO-CPHF, GIAO-SCF and GIAO-DFT (UDFT-GIAO-BPW91 and GIAO-B3LYP) were employed to calculate the chemical shifts.^[11] Our research group has found that the GIAO-B3LYP//3-21G and GIAO-HF//3-21G methods with AM1- or PM3-optimized geometries exhibit a very good linear relationship between calculated and experimental ^3He chemical shifts of endofullerenes and further applied these methods to the prediction and assignment of ^3He -encapsulated fullerenes and fullerene derivatives.^[12] As a continuation of our interest in fullerene chemistry,^[12,13] we report herein the accurate calculation and prediction of the endohedral ^1H NMR chemical shifts of H_2 -, H_2O - and NH_3 -encapsulated fullerene compounds.

Computational Details

The geometries of H_2 -, H_2O - and NH_3 -encapsulated fullerene compounds and tetramethylsilane (TMS), H_2 , H_2O and NH_3 were optimized without symmetry constraint at the semiempirical AM1^[14] and/or PM3^[15] levels. The chemical shifts were calculated at the GIAO (gauge including atomic orbitals^[16])-HF and/or GIAO-B3LYP (Becke's^[17] three-parameter hybrid-exchange functional and the corre-

[a] Hefei National Laboratory for Physical Sciences on Microscale and Department of Chemistry, University of Science and Technology of China, Hefei, Anhui, 230026, People's Republic of China
Fax: +86-551-360-7864
E-mail: gwang@ustc.edu.cn

lation functional of Lee et al.^[18]) levels with the 3-21G basis set. The calculated endohedral ¹H NMR chemical shifts (δ_{calc}) are given in ppm relative to the ¹H NMR chemical shift of TMS. The calculated chemical shifts of TMS are 33.10, 33.60, 32.63 and 33.14 ppm at the GIAO-HF/3-21G//AM1, GIAO-HF/3-21G//PM3, GIAO-B3LYP/3-21G//AM1 and GIAO-B3LYP/3-21G//PM3 levels, respectively. The chemical shifts calculated for H₂ are 28.57 and 28.07 ppm at the GIAO-B3LYP/3-21G//AM1 and GIAO-B3LYP/3-21G//PM3 levels, respectively. The corrected chemical shifts (δ_{corr})^[19] were obtained from the correlation equation derived from the linear regression fitting between calculated and experimental ¹H NMR chemical shifts in each case. All calculations were carried out with the help of the GAUSSIAN 03 program package.^[20]

Results and Discussion

Unlike a helium atom encapsulated in fullerenes, a hydrogen, water or ammonia molecule has two or three hydrogen atoms inside a fullerene compound. Under common conditions, because of their free movement in fullerene cages, the hydrogen atoms of molecular hydrogen, water or ammonia should exhibit the same chemical shift, which has been confirmed by experimental results. However, because of the unconstrained symmetry in computational methods, the hydrogen atoms should undoubtedly display different chemical shifts. To evaluate the influence of different orientations of the encapsulated molecules, we chose H₂@C₆₀C₆H₄ (**1**) as an example to address this problem. Three representative orientations were selected and are illustrated as **1a**, **1b** and **1c** in Figure 1. As shown by the results of calculations (Table 1), the chemical shifts of the two protons in **1a** and **1b** are nearly the same: –5.81 and –5.84 ppm for **1a**, –5.83 and –5.85 ppm for **1b** at the GIAO-HF/3-21G//PM3 level; –0.27 and –0.30 ppm for **1a**, –0.32 and –0.34 ppm for **1b** at the GIAO-B3LYP/3-21G//PM3 level. As for **1c**, the calculated chemical shifts of the two protons show a large deviation. The main reason for this should arise from the unsymmetrical locations of the two hydrogen atoms in **1c**. However, the average chemical shift of these two protons is close to those in **1a** and **1b** (to within 0.10 ppm). The relative energies of **1a**, **1b** and **1c** are 0.01, 0.00 and 0.01 kcalmol^{–1} at both the AM1 and PM3 levels, respectively. For this reason, we decided to choose the most stable structures for the NMR calculations and the resulting average endohedral chemical shifts as the calculated chemical shifts.

Endohedral ¹H NMR Calculations of Various Fullerene Compounds by Different Methods

Calculations were carried out on H₂@C₆₀ (**2**), H₂-encapsulated closed-cage [60]fullerene derivatives **1** and **3–8**, such as monoadducts with a three-membered ring (**3**), a four-membered ring (**1**), a five-membered ring (**4**), the dimer (H₂@C₆₀)₂ (**5**) and C₆₀ multiadducts **6–8**, H₂-encapsulated

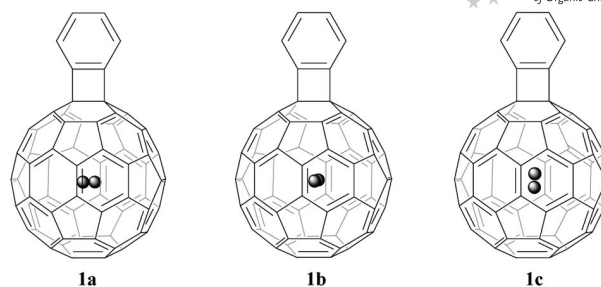


Figure 1. Three representative orientations of H₂ in compound **1**.

Table 1. Chemical shifts calculated at the GIAO-HF/3-21G and GIAO-B3LYP/3-21G levels of theory with the geometries optimized by the PM3 method.

	δ (ppm)					
	GIAO-HF/3-21G//PM3			GIAO-B3LYP/3-21G//PM3		
	H-1	H-2	Average	H-1	H-2	Average
1a	–5.81	–5.84	–5.83	–0.27	–0.30	–0.29
1b	–5.83	–5.85	–5.84	–0.32	–0.34	–0.33
1c	–5.44	–6.06	–5.75	–0.50	0.02	–0.24

open-cage [60]fullerenes with eight- to sixteen-membered-ring orifices (**9–20**), as well as H₂-encapsulated open-cage [70]fullerene compounds with a thirteen-membered-ring orifice (**21** and **22**) (Figure 2). A few H₂O-encapsulated open-cage [60]fullerenes with fifteen- to seventeen-membered-ring orifices (**23–30**) and a recently reported NH₃-encapsulated open-cage fullerene (**31**) were also included. All compounds were optimized by the AM1 and PM3 semiempirical methods at nearly the same computational cost. The endohedral ¹H NMR chemical shifts were calculated for compounds **1–31** at the GIAO-B3LYP/3-21G and GIAO-HF/3-21G levels of theory by using both the AM1- and PM3-optimized geometries.

The linear regression fittings between the calculated and experimental chemical shifts are shown in Figures 3, 4, 5, and 6. The correlation equation between the corrected and experimental chemical shifts along with the regression coefficient (*R*) and standard deviation (*SD*) are shown in each figure. The calculated chemical shifts (δ_{calc}), corrected chemical shifts (δ_{corr}) and experimental shifts (δ_{exp}) are listed in Table 2.

As judged by the regression coefficients and standard deviations shown in Figures 3–6, the chemical shifts calculated by the GIAO-B3LYP/3-21G method have clear advantages over those calculated by the GIAO-HF/3-21G method. With the AM1- and PM3-optimized geometries, the regression coefficients given by the GIAO-B3LYP/3-21G method are –0.953 and –0.985, respectively, whereas the corresponding regression coefficients by the GIAO-HF/3-21G method are –0.845 and –0.958. For the PM3-optimized geometries, the maximum errors in the corrected chemical shifts at the GIAO-B3LYP/3-21G and GIAO-HF/3-21G levels (shown in Table 2) are 1.59 and 2.70 ppm, respectively, whereas the mean errors are 0.56 and 0.83 ppm. In comparison, for the AM1-optimized geometries the corresponding maximum errors are 2.70 and

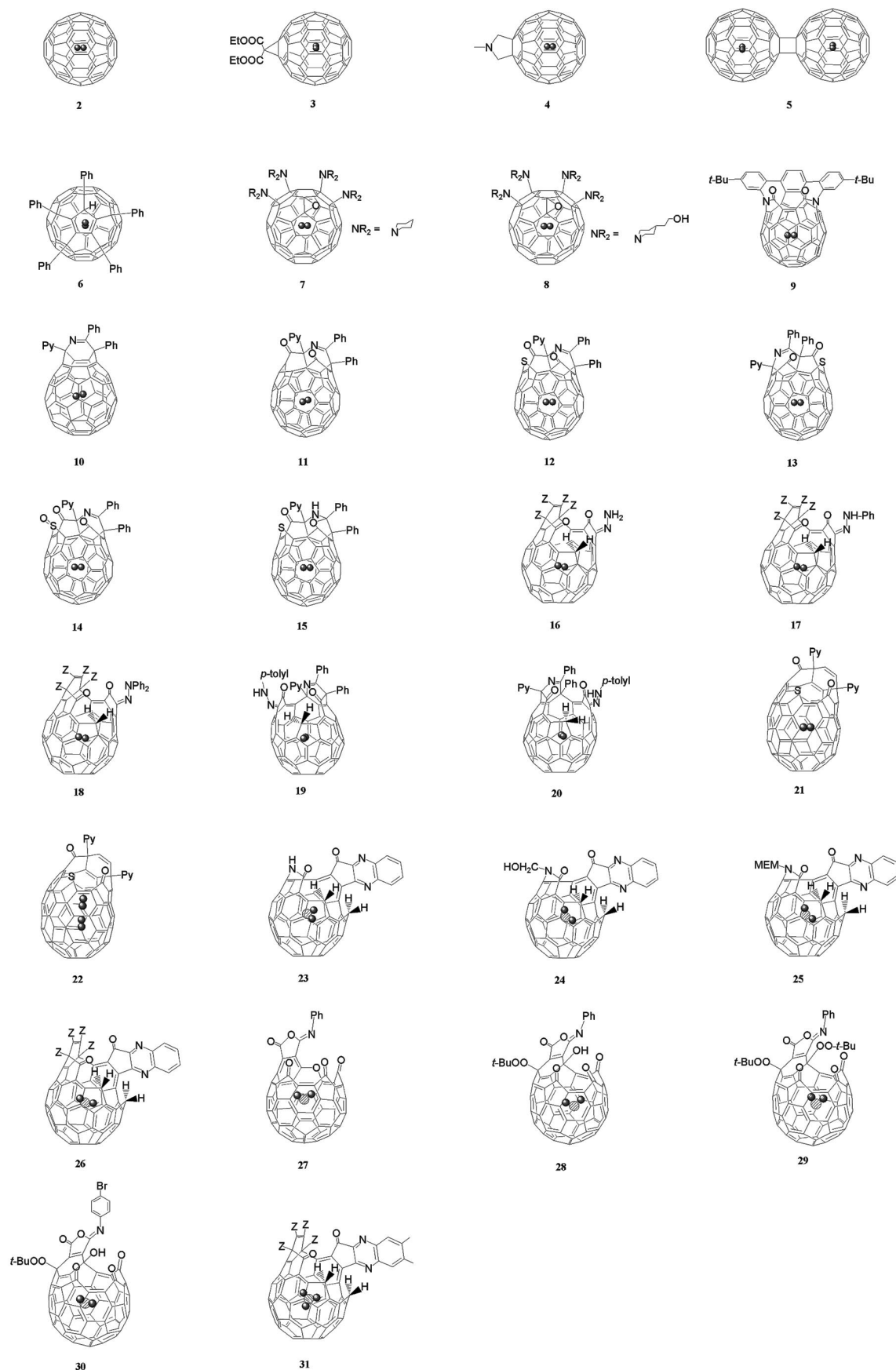


Figure 2. Structures of endofullerene compounds 2–31 (Z = COOMe, Py = 2-pyridine; ●: hydrogen atom; ○: oxygen atom; ⊙: nitrogen atom).

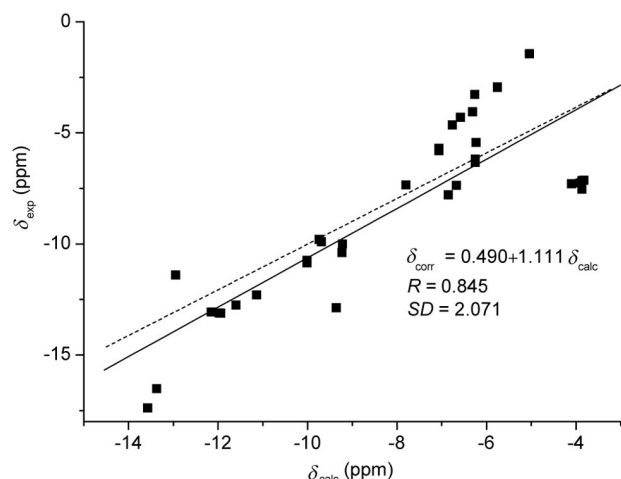


Figure 3. The linear fitting between δ_{exp} and δ_{calc} (calculated at the GIAO-HF/3-21G//AM1 level) for compounds 1–31. The dashed line represents the fitting for a slope and y intercept of 1 and 0, respectively.

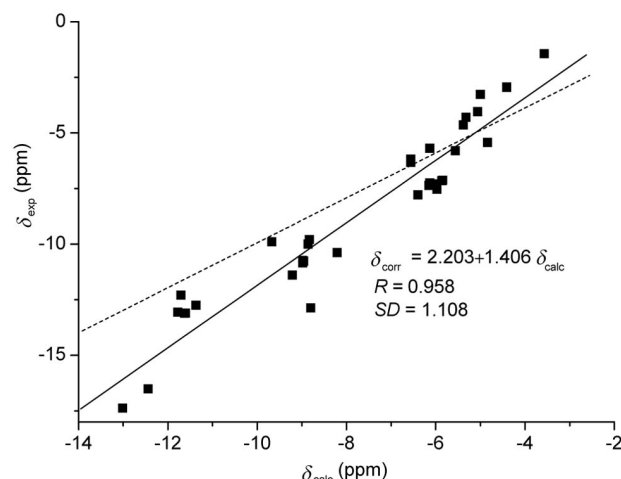


Figure 4. The linear fitting between δ_{exp} and δ_{calc} (calculated at the GIAO-HF/3-21G//PM3 level) for compounds 1–31. The dashed line represents the fitting for a slope and y intercept of 1 and 0, respectively.

3.72 ppm and the respective mean errors are 0.96 and 1.53 ppm. By comparison of the regression coefficients, standard deviations and maximum and mean errors of the corrected chemical shifts, it can be concluded that of the four employed methods the GIAO-B3LYP/3-21G//PM3 method is the best one for calculating the endohedral ¹H NMR shifts of endofullerenes. For geometries optimized at the PM3 level, most of the corrected chemical shifts given by the GIAO-B3LYP/3-21G method are very close, within 1.00 ppm, to the experimental results. The correlation equation between the calculated and corrected chemical shifts by the GIAO-B3LYP/3-21G//PM3 method is shown in Equation (1).

$$\delta_{\text{corr}} = -4.125 + 1.038\delta_{\text{calc}} \quad (1)$$

To demonstrate the efficiency and accuracy of our GIAO-B3LYP/3-21G//PM3 method, $\text{H}_2@\text{C}_{60}$ is used as an

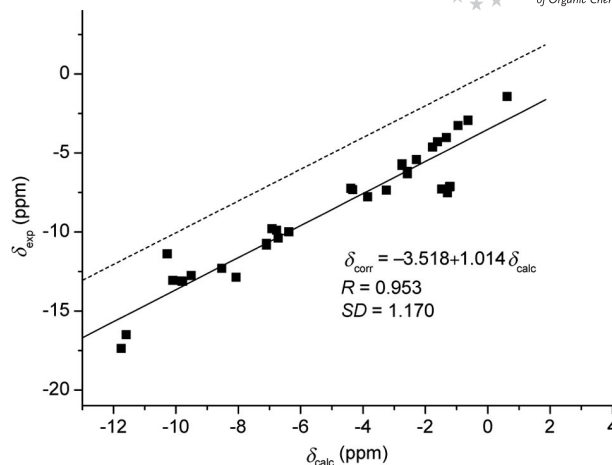


Figure 5. The linear fitting between δ_{exp} and δ_{calc} (calculated at the GIAO-B3LYP/3-21G//AM1 level) for compounds 1–31. The dashed line represents the fitting for a slope and y intercept of 1 and 0, respectively.

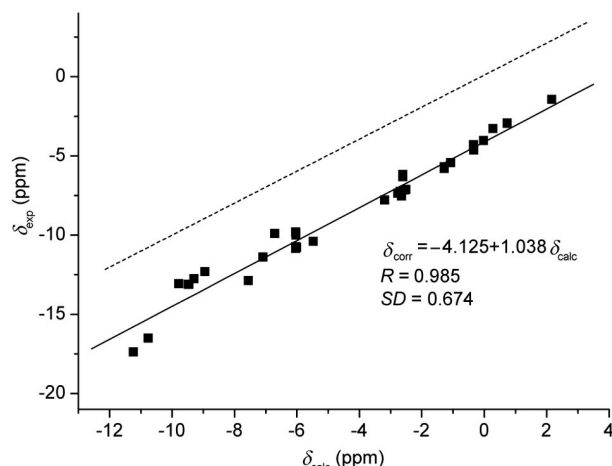


Figure 6. The linear fitting between δ_{exp} and δ_{calc} (calculated at the GIAO-B3LYP/3-21G//PM3 level) for compounds 1–31. The dashed line represents the fitting for a slope and y intercept of 1 and 0, respectively.

example. The theoretical prediction of the endohedral chemical shift of $\text{H}_2@\text{C}_{60}$ at the GIAO-B3LYP/6-311G*//B3LYP/6-31G* level is 1.79 ppm,^[6b] which is a deviation from the experimentally obtained −1.45 ppm^[6] of 3.24 ppm. However, the corrected chemical shift for $\text{H}_2@\text{C}_{60}$ by our method is −1.88 ppm, which is close to the experimental value.

The endohedral ¹H NMR chemical shift for any unreported H_2 -, H_2O - or NH_3 -encapsulated endofullerene can be quickly and accurately predicted by the GIAO-B3LYP/3-21G//PM3 method by using Equation (1). It is clear that calculations of the endohedral ¹H NMR chemical shifts of a new endofullerene by our method would consume much less computational time than the existing GIAO-B3LYP/6-311G*//B3LYP/6-31G* method and is still expected to provide a good prediction of the endohedral chemical shift.

Table 2. Calculated, corrected and experimental ^1H NMR chemical shifts (in ppm) and statistical data for the ^1H NMR chemical shifts encapsulated in compounds 1–31.

	GIAO-HF/3-21G				GIAO-B3LYP/3-21G				δ_{exp}
	AM1 δ_{calc}	δ_{corr}	PM3 δ_{calc}	δ_{corr}	AM1 δ_{calc}	δ_{corr}	PM3 δ_{calc}	δ_{corr}	
1	-6.58	-6.82	-5.32	-5.28	-1.61	-5.15	-0.34	-4.47	-4.30 ^[a]
2	-5.04	-5.11	-3.57	-2.81	0.62	-2.89	2.16	-1.88	-1.44 ^[a]
3	-6.26	-6.46	-5.00	-4.83	-0.95	-4.49	0.28	-3.84	-3.27 ^[a]
4	-6.76	-7.02	-5.38	-5.37	-1.77	-5.32	-0.33	-4.47	-4.64 ^[a]
5	-6.31	-6.53	-5.06	-4.91	-1.33	-4.86	-0.02	-4.15	-4.04 ^[a]
6	-9.23	-9.77	-8.21	-9.34	-6.72	-10.33	-5.48	-9.81	-10.39 ^[b]
7	-10.01	-10.63	-8.96	-10.40	-7.10	-10.72	-6.01	-10.36	-10.77 ^[b]
8	-10.01	-10.63	-8.98	-10.42	-7.10	-10.72	-6.04	-10.39	-10.74, ^[b] -10.76, ^[b] -10.80, ^[b] -10.85 ^[b]
9	-6.23	-6.43	-4.84	-4.60	-2.29	-5.84	-1.07	-5.23	-5.43 ^[c]
10	-5.76	-5.91	-4.41	-4.00	-0.63	-4.15	0.73	-3.36	-2.95, ^[a] -2.93 ^[d]
11	-7.06	-7.35	-5.56	-5.62	-2.75	-6.31	-1.28	-5.45	-5.80, ^[a] -5.69 ^[d]
12	-3.91	-3.85	-6.13	-6.42	-4.39	-7.97	-2.69	-6.92	-7.25 ^[e]
13	-6.67	-6.92	-6.15	-6.45	-3.25	-6.81	-2.77	-7.00	-7.36 ^[f]
14	-6.25	-6.46	-6.56	-7.02	-2.58	-6.13	-2.61	-6.84	-6.33, ^[a] -6.18 ^[d]
15	-6.85	-7.12	-6.40	-6.80	-3.85	-7.42	-3.19	-7.44	-7.79 ^[g]
16	-7.80	-8.18	-5.98	-6.21	-4.33	-7.91	-2.67	-6.89	-7.34 ^[h]
17	-3.87	-3.81	-5.97	-6.20	-1.29	-4.83	-2.65	-6.87	-7.53 ^[h]
18	-4.10	-4.07	-6.01	-6.24	-1.48	-5.02	-2.64	-6.87	-7.29 ^[h]
19	-3.87	-3.81	-5.86	-6.03	-1.22	-4.76	-2.55	-6.78	-7.15 ^[i]
20	-3.82	-3.75	-5.84	-6.00	-1.21	-4.74	-2.51	-6.73	-7.13 ^[i]
21	-13.37	-14.36	-12.44	-15.28	-11.59	-15.27	-10.76	-15.30	-16.51 ^[i]
22	-9.36	-9.91	-8.80	-10.17	-8.07	-11.70	-7.56	-11.97	-12.87 ^[i]
22	-13.57	-14.59	-13.01	-16.09	-11.75	-15.43	-11.24	-15.79	-17.38 ^[i]
23	-9.69	-10.28	-9.67	-11.39	-6.77	-10.39	-6.71	-11.09	-9.90 ^[j]
24	-9.74	-10.33	-8.83	-10.22	-6.92	-10.53	-6.04	-10.39	-9.80 ^[j]
25	-9.22	-9.75	-8.86	-10.26	-6.38	-9.99	-6.03	-10.39	-10.00 ^[j]
26	-12.95	-13.90	-9.21	-10.75	-10.28	-13.94	-7.09	-11.48	-11.40 ^[k]
27	-11.60	-12.40	-11.37	-13.78	-9.51	-13.16	-9.30	-13.78	-12.75 ^[l]
28	-11.98	-12.82	-11.61	-14.12	-9.82	-13.47	-9.48	-13.97	-13.11 ^[l]
29	-12.15	-13.01	-11.78	-14.36	-10.10	-13.76	-9.79	-14.29	-13.07 ^[l]
30	-11.94	-12.77	-11.63	-14.14	-9.79	-13.44	-9.46	-13.95	-13.12 ^[l]
31	-11.14	-11.88	-11.71	-14.26	-8.53	-12.17	-8.95	-13.42	-12.30 ^[m]
Mean error		1.53		0.96		0.83		0.56	
Max. error		3.72		2.70		2.70		1.59	

[a] Ref.^[6b] [b] Ref.^[21] [c] Ref.^[4a] [d] Ref.^[6a] [e] Ref.^[5a] [f] Ref.^[5d] [g] Ref.^[4c] [h] Ref.^[5b] [i] Ref.^[5c] [j] Ref.^[7b] [k] Ref.^[7a] [l] Ref.^[7c] [m] Ref.^[9]

Prediction of Endohedral ^1H NMR Chemical Shifts

Even though the synthesis of $\text{H}_2@\text{C}_{60}$ has been successfully achieved by a multistep process, H_2 -encapsulated higher fullerenes such as $\text{H}_2@\text{C}_{70}$ are still waiting to be made. Similarly, the preparation of $\text{H}_2\text{O}@\text{C}_{60}$, $\text{H}_2\text{O}@\text{C}_{70}$, $\text{NH}_3@\text{C}_{60}$ and $\text{NH}_3@\text{C}_{70}$ is an even more challenging task. However, their endohedral ^1H NMR chemical shifts would be of great interest to chemists.

We therefore would like to predict the endohedral ^1H NMR chemical shifts of various as-yet-unreported endofullerenes. These unknown H_2 -encapsulated higher fullerenes and their derivatives include $\text{H}_2@\text{C}_{70}$ (**32**), $\text{H}_2@\text{C}_{76}$ (**33**), three isomers of $\text{H}_2@\text{C}_{78}$ (**34–36**), $\text{H}_2@\text{C}_{70}\text{H}_2$ (**37**), $\text{H}_2@\text{C}_{70}\text{H}_4$ (**38**), $\text{H}_2@\text{C}_{70}\text{H}_8$ (**39**) and $\text{H}_2@\text{C}_{70}\text{H}_{10}$ (**40**). H_2 -encapsulated heterofullerenes include $\text{H}_2@\text{C}_{59}\text{N}^+$ (**41**), $\text{H}_2@\text{C}_{59}\text{NH}$ (**42**), $\text{H}_2@\text{C}_{57}\text{N}_3^{3+}$ (**43**), $\text{H}_2@\text{C}_{57}\text{N}_3\text{H}_3$ (**44**), two isomers of $\text{H}_2@\text{C}_{69}\text{N}^+$ (**45** and **46**) and two isomers of $\text{H}_2@\text{C}_{69}\text{NH}$ (**47** and **48**). H_2O - and NH_3 -encapsulated fullerenes include $\text{H}_2\text{O}@\text{C}_{60}$ (**49**), $\text{H}_2\text{O}@\text{C}_{70}$ (**50**), $\text{NH}_3@\text{C}_{60}$ (**51**) and $\text{NH}_3@\text{C}_{70}$ (**52**). $\text{H}_2@\text{C}_{60}\text{H}_2$ (**53**) is in-

cluded for comparison (Figure 7). The endohedral ^1H NMR chemical shifts of these compounds were calculated by the GIAO-B3LYP/3-21G//PM3 method and the corresponding corrected chemical shifts were generated from Equation (1). The calculated and corrected chemical shifts are collected in Table 3.

By comparison of the corrected chemical shifts (δ_{corr}) of the H_2 -encapsulated fullerene compounds (**1–22**, **32–40**) in Table 2 and Table 3, it can be seen that the δ_{corr} values for $\text{H}_2@\text{C}_{60}$ and $\text{H}_2@\text{C}_{70}$ are located at two extremes, and that all the other δ_{corr} values, including those of the derivatives of $\text{H}_2@\text{C}_{60}$ and $\text{H}_2@\text{C}_{70}$ as well as the higher fullerenes $\text{H}_2@\text{C}_{76}$ and $\text{H}_2@\text{C}_{78}$, lie between the two extremes. For H_2 -encapsulated closed-cage [60]fullerene monoadducts, δ_{corr} exhibits an upfield shift relative to that of $\text{H}_2@\text{C}_{60}$, increasing gradually from the monoadduct with a three-membered ring (**3**) to the monoadduct with a five-membered-ring (**4**). The δ_{corr} values show an even more drastic upfield shift for the H_2 -encapsulated multiadducts of C_{60} (**6–8**). The δ_{corr} values for open-cage [60]fullerene derivatives **9–20** also display a significant upfield shift compared

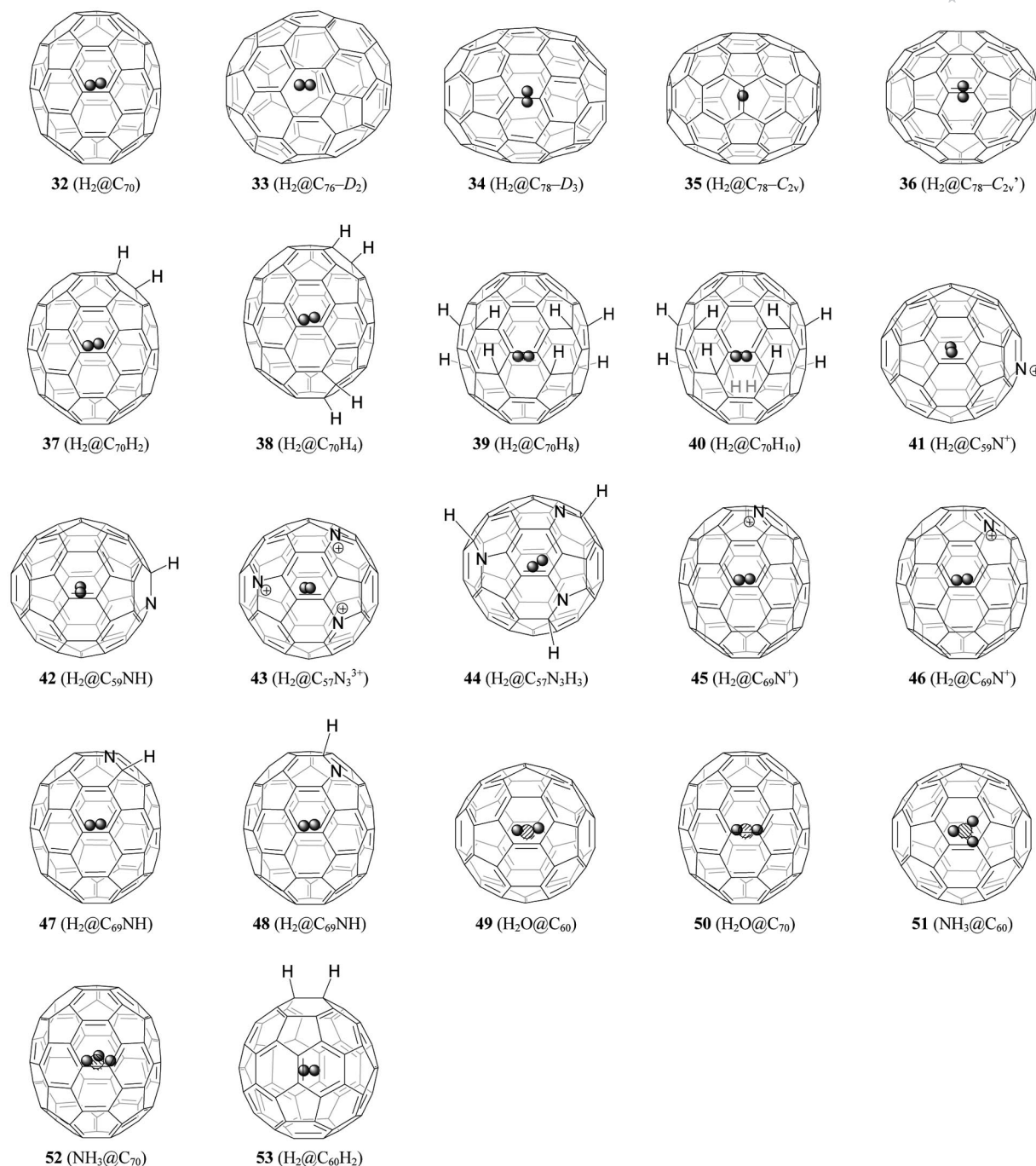


Figure 7. Structures of H_2 -encapsulated fullerene compounds **32–53** (●: hydrogen atom; ●: oxygen atom; ●: nitrogen atom).

with that of $\text{H}_2@C_{60}$. In sharp contrast, the δ_{corr} values for [70]fullerene derivatives with open- (**21** and **22**) or closed-cage structures (**37–40**) demonstrate a downfield shift relative to that of $\text{H}_2@C_{70}$. The above phenomena have also been observed in the endohedral ^3He NMR chemical shifts of fullerene compounds.^[22]

The H_2 -encapsulated heterofullerenes show some interesting and unexpected endohedral chemical shift behaviour compared with their unsubstituted parent fullerenes. The δ_{corr} data for $\text{H}_2@C_{59}N^+$ and its derivative are slightly downfield-shifted compared with the parent fullerenes ($\delta =$

-1.83 ppm for $\text{H}_2@C_{59}N^+$ vs. -1.88 ppm for $\text{H}_2@C_{60}$, -4.49 ppm for $\text{H}_2@C_{59}NH$ vs. -4.72 ppm for $\text{H}_2@C_{60}H_2$). The recently reported triazafullerene $C_{57}N_3$ ^[23] is more likely to exist as $C_{57}N_3^{3+}$ or $C_{57}N_3H_3$. The calculated δ_{corr} for $\text{H}_2@C_{57}N_3^{3+}$ is -0.78 ppm, and is shifted further downfield than for $\text{H}_2@C_{59}N^+$. The calculated δ_{corr} for $\text{H}_2@C_{57}N_3H_3$ ($\delta = -10.13$ ppm) is quite different from that of $\text{H}_2@C_{57}N_3^{3+}$ and thus the actually formed species could easily be distinguished by their endohedral ^1H NMR chemical shifts. One $\text{H}_2@C_{69}N^+$ isomer (**45**) has a more downfield chemical shift than $\text{H}_2@C_{70}$, whereas another

Table 3. Calculated (δ_{calc}) and corrected (δ_{corr}) chemical shifts for compounds **32–53**.

Species	δ_{calc} (ppm)	δ_{corr} (ppm)
32 ($\text{H}_2@C_{70}$)	–15.41	–20.12
33 ($\text{H}_2@C_{76}-D_2$)	–7.96	–12.39
34 ($\text{H}_2@C_{78}-D_3$)	–2.04	–6.25
35 ($\text{H}_2@C_{78}-C_{2v}$)	–6.50	–10.88
36 ($\text{H}_2@C_{78}-C_{2v}'$)	–6.63	–11.00
37 ($\text{H}_2@C_{70}\text{H}_2$)	–14.68	–19.36
38 ($\text{H}_2@C_{70}\text{H}_4$)	–13.65	–18.29
39 ($\text{H}_2@C_{70}\text{H}_8$)	–7.51	–11.92
40 ($\text{H}_2@C_{70}\text{H}_{10}$)	–7.26	–11.66
41 ($\text{H}_2@C_{59}\text{N}^+$)	2.21	–1.83
42 ($\text{H}_2@C_{59}\text{NH}$)	–0.35	–4.49
43 ($\text{H}_2@C_{57}\text{N}_3^{3+}$)	3.22	–0.78
44 ($\text{H}_2@C_{57}\text{N}_3\text{H}_3$)	–5.78	–10.13
45 ($\text{H}_2@C_{69}\text{N}^+$)	–12.98	–17.59
46 ($\text{H}_2@C_{69}\text{N}^+$)	–15.56	–20.28
47 ($\text{H}_2@C_{69}\text{NH}$)	–13.66	–18.30
48 ($\text{H}_2@C_{69}\text{NH}$)	–15.66	–20.38
49 ($\text{H}_2\text{O}@C_{60}$)	–3.15	–7.39
50 ($\text{H}_2\text{O}@C_{70}$)	–20.59	–25.50
51 ($\text{NH}_3@C_{60}$)	–4.09	–8.37
52 ($\text{NH}_3@C_{70}$)	–21.46	–26.40
53 ($\text{H}_2@C_{60}\text{H}_2$)	–0.57	–4.72

$\text{H}_2@C_{69}\text{N}^+$ isomer (**46**) exhibits a shift in the reverse direction. Similar trends in the chemical shifts can also be seen for $\text{H}_2@C_{69}\text{NH}$: one isomer is more downfield-shifted and another one is more upfield-shifted than $\text{H}_2@C_{70}\text{H}_2$. In contrast to the derivatives of $\text{H}_2@C_{70}$, the derivatives of both $\text{H}_2@C_{69}\text{N}^+$ isomers display upfield shifts (–18.30 and –20.38 ppm for $\text{H}_2@C_{69}\text{NH}$ vs. –17.59 and –20.28 ppm for $\text{H}_2@C_{69}\text{N}^+$, respectively). These results indicate that substitution of carbon atom(s) in fullerenes by nitrogen atom(s) has a noticeable effect on the endohedral ^1H NMR chemical shifts.

The endohedral chemical shifts also strongly depend on the orifice sizes of the open-cage fullerene compounds, as can be seen in compounds **9–20**. The larger the orifice size is, the more upfield the endohedral chemical shift. Nevertheless, the δ_{corr} value is little affected by the addends of endofullerenes with the same addition pattern and/or fullerene motif, for example, around –10 ppm for the H_2 -encapsulated multiadducts **6–8**, around –7 ppm for H_2 -encapsulated open-cage compounds **16–18** and around –14 ppm for H_2O -encapsulated open-cage compounds **28–30**.

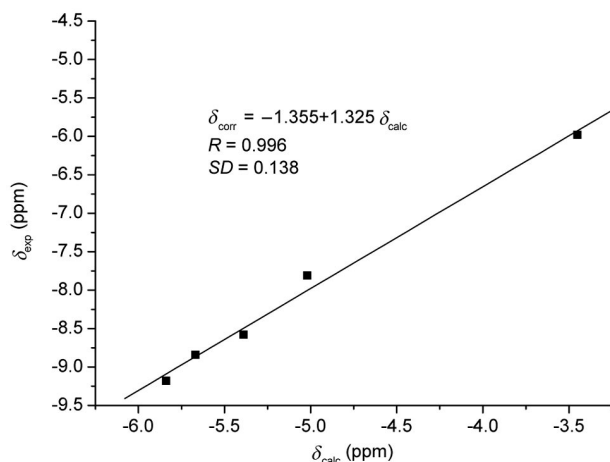
Note that the endohedral ^1H NMR chemical shifts of H_2 , H_2O and NH_3 in a fullerene cage gradually move upfield. For example, the δ_{corr} values for $\text{H}_2@C_{60}$, $\text{H}_2\text{O}@C_{60}$ and $\text{NH}_3@C_{60}$ are –1.88, –7.39 and –8.37 ppm, meanwhile those for $\text{H}_2@C_{70}$, $\text{H}_2\text{O}@C_{70}$ and $\text{NH}_3@C_{70}$ are –20.12, –25.50 and –26.40 ppm. A 5.51 ppm upfield shift is seen from $\text{H}_2@C_{60}$ to $\text{H}_2\text{O}@C_{60}$, and nearly the same value ($\delta = 5.38$ ppm) is found from $\text{H}_2@C_{70}$ to $\text{H}_2\text{O}@C_{70}$. Changing the encapsulated molecule from H_2O to NH_3 leads to an additional upfield shift, that is, 0.98 and 0.90 ppm for C_{60} and C_{70} , respectively. The computed corrected chemical shifts for H_2 , H_2O and NH_3 are 1.13, –4.47 and –5.24 ppm by the GIAO-B3LYP/3-21G//PM3 method, that is the same

trend and comparable chemical shift differences (5.61 and 0.77 ppm, respectively) as the encapsulated species. The endohedral ^1H NMR chemical shift differences for $\text{H}_2@C_{60}$, $\text{H}_2\text{O}@C_{60}$ and $\text{NH}_3@C_{60}$ relative to the corresponding free guest molecule are 3.01, 2.92 and 3.13 ppm, whereas those for $\text{H}_2@C_{70}$, $\text{H}_2\text{O}@C_{70}$ and $\text{NH}_3@C_{70}$ are 21.25, 21.03 and 21.16 ppm. Therefore, the fullerene skeleton of either C_{60} or C_{70} has nearly the same shielding effect on the encapsulated molecules.

Comparison Between Endohedral ^1H and ^3He NMR Chemical Shifts

With the aim of better understanding the endohedral chemical shifts of the encapsulated molecule in fullerene compounds, we attempted to find the relationship between the endohedral ^1H and ^3He NMR chemical shifts with the free molecule as reference. Only five fullerene compounds encapsulating either H_2 or ^3He have experimental data for both endohedral ^1H and ^3He NMR chemical shifts relative to the corresponding dissolved free molecule. For the H_2 -encapsulated fullerene compounds, these are compounds **1–5**. We name the ^3He counterparts as compounds **54–58**.

Both the GIAO-B3LYP/3-21G//AM1 and GIAO-B3LYP/3-21G//PM3 methods were employed to calculate the endohedral ^1H and ^3He NMR chemical shifts. The linear regression fittings between calculated and experimental chemical shifts for compounds **1–5** relative to free H_2 and those for compounds **54–58** relative to free ^3He are shown in Figures 8, 9, 10 and 11. The δ_{calc} , δ_{corr} and δ_{exp} values for compounds **1–5** relative to free H_2 and those for compounds **54–58** relative to free ^3He are listed in Table 4.

Figure 8. The linear fitting between δ_{exp} and δ_{calc} (calculated at the GIAO-B3LYP/3-21G//AM1 level) for compounds **1–5** relative to free H_2 .

As can be seen from Figures 8–11 and Table 4, the two methods provide excellent correlation between δ_{corr} and δ_{exp} for both series (compounds **1–5** vs. compounds **54–58**). Furthermore, the δ_{corr} and δ_{exp} values for compounds **1–5**

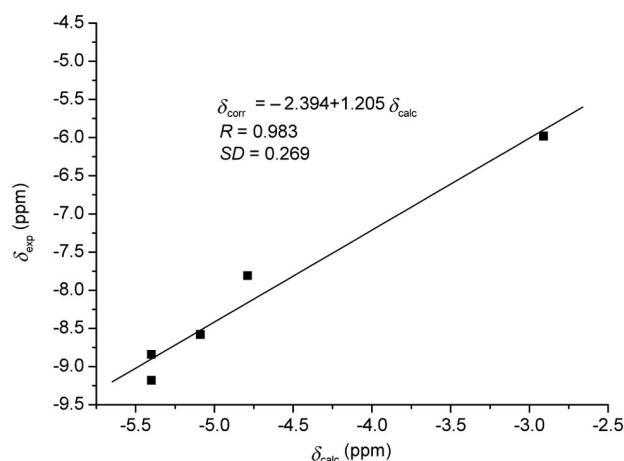


Figure 9. The linear fitting between δ_{exp} and δ_{calc} (calculated at the GIAO-B3LYP/3-21G//PM3 level) for compounds **1–5** relative to free H_2 .

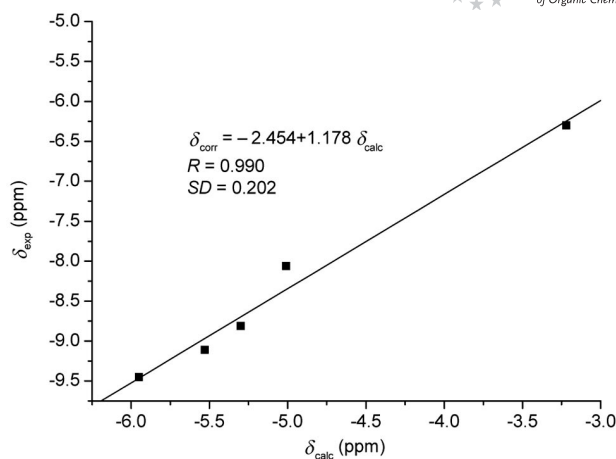


Figure 11. The linear fitting between δ_{exp} and δ_{calc} (calculated at the GIAO-B3LYP/3-21G//PM3 level) for compounds **54–58** relative to free ^3He .

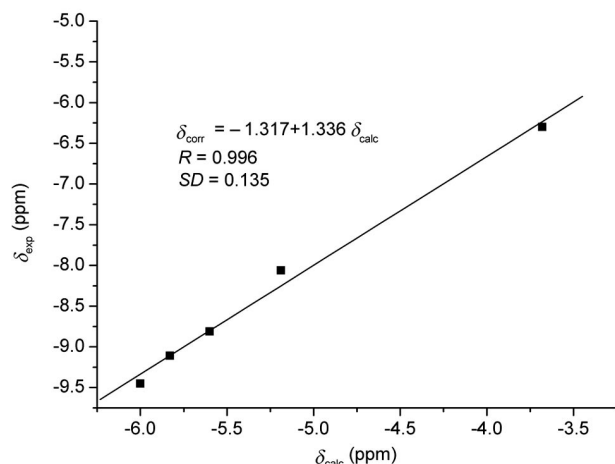


Figure 10. The linear fitting between δ_{exp} and δ_{calc} (calculated at the GIAO-B3LYP/3-21G//AM1 level) for compounds **54–58** relative to free ^3He .

relative to free H_2 are very close to those of compounds **54–58** relative to free ^3He , which indicates that the fullerene skeleton has a similar magnetic effect on both the encapsulated H_2 and ^3He .

In our previous work on endohedral ^3He NMR calculations, our data demonstrated that the δ_{corr} values for $^3\text{He}@C_{60}$ and $^3\text{He}@C_{70}$ calculated by the GIAO-B3LYP/3-21G//PM3 and GIAO-B3LYP/3-21G//AM1 methods are very close to the experimental values.^[12] The δ_{corr} difference between $^3\text{He}@C_{60}$ and $^3\text{He}@C_{70}$ is 22.66 ppm at the GIAO-B3LYP/3-21G//PM3 level and 22.75 ppm at the GIAO-B3LYP/3-21G//AM1 level, nearly identical to the δ_{exp} difference ($\delta = 22.50$ ppm).^[12] As shown in Table 2, the δ_{corr} values for H_2 -, H_2O - and NH_3 -encapsulated endofullerenes coincide with their experimental δ_{exp} data, and the δ_{corr} difference between H_2 -encapsulated C_{60} and C_{70} is 18.24 ppm, close to 18.11 and 18.03 ppm for the H_2O - and NH_3 -encapsulated C_{60} and C_{70} . The similarly large chemical shift difference between encapsulated C_{60} and C_{70} indicates that the endohedral He, H_2 , H_2O and NH_3 are excellent indicators of the magnetic properties of the fullerene skeleton. Thus, an encapsulated H_2 , H_2O or NH_3 molecule can also be a sensitive and powerful NMR probe for exploring the ring currents of the fullerene cages.

Conclusions

Endohedral ^1H NMR chemical shifts of various reported H_2 - H_2O - and NH_3 -encapsulated fullerene compounds have been calculated at the GIAO-B3LYP/3-21G and GIAO-HF/

Table 4. Calculated (δ_{calc}), corrected (δ_{corr}) and experimental (δ_{exp}) chemical shifts (in ppm) for compounds **1–5** and **54–58**.

Species	B3LYP/3-21G//AM1		B3LYP/3-21G//PM3		δ_{exp}	Species	B3LYP/3-21G//AM1		B3LYP/3-21G//PM3		δ_{exp}
	δ_{calc}	δ_{corr}	δ_{calc}	δ_{corr}			δ_{calc}	δ_{corr}	δ_{calc}	δ_{corr}	
1	−5.67	−8.87	−5.40	−8.90	−8.84 ^[a]	54	−5.83 ^[b]	−9.11	−5.53 ^[b]	−8.97	−9.11 ^[c]
2	−3.45	−5.92	−2.91	−5.90	−5.98 ^[a]	55	−3.68 ^[b]	−6.23	−3.22 ^[b]	−6.25	−6.30 ^[d]
3	−5.02	−8.01	−4.79	−8.16	−7.81 ^[a]	56	−5.19 ^[b]	−8.25	−5.01 ^[b]	−8.36	−8.06 ^[c]
4	−5.84	−9.09	−5.40	−8.90	−9.18 ^[a]	57	−6.00 ^[b]	−9.33	−5.95 ^[b]	−9.46	−9.45 ^[c]
5	−5.39	−8.50	−5.09	−8.53	−8.58 ^[a]	58	−5.60	−8.80	−5.30	−8.70	−8.81 ^[e]

[a] Ref.^[6b] [b] Data taken from ref.^[12] [c] Ref.^[3c] [d] Ref.^[3b] [e] Ref.^[24]

3-21G levels of theory with AM1- and PM3-optimized geometries. The linear regression fitting of the calculated and experimental chemical shifts for each of the four methods yields regression coefficients and standard deviations that indicate that the GIAO-B3LYP/3-21G method is better than the GIAO-HF/3-21G method. The corrected ^1H NMR chemical shifts were calculated from the correlation equation in each case. By comparing the regression coefficients, standard deviations and maximum and mean errors of the corrected chemical shifts obtained by the four employed methods, it can be concluded that the GIAO-B3LYP/3-21G//PM3 method is the best one for calculating the endohedral ^1H NMR chemical shifts of endofullerenes. The corrected chemical shifts given by the GIAO-B3LYP/3-21G//PM3 method are close to the experimental values, mostly within 1.00 ppm. For any interesting as-yet-unreported H_2 -, H_2O - or NH_3 -encapsulated fullerene compound the endohedral ^1H NMR chemical shifts can be predicted by the correlation equation established by the GIAO-B3LYP/3-21G//PM3 method. The chemical shifts calculated are expected to apply to the structural assignments of H_2 -, H_2O - or NH_3 -encapsulated fullerenes and their derivatives. Generally, H_2 -encapsulated [60]fullerene derivatives with both closed- and open-cage structures show upfield endohedral chemical shifts relative to $\text{H}_2@C_{60}$. In contrast, those of [70]fullerene derivatives exhibit downfield endohedral chemical shifts relative to $\text{H}_2@C_{70}$. Similar phenomena have also been observed in the shift tendency of the endohedral ^3He chemical shifts of ^3He -encapsulated fullerene compounds. Nitrogen-substituted heterofullerenes and their derivatives display intriguing endohedral chemical shifts compared with their parent fullerenes and should be of great interest and deserve further experimental studies. Just like the encapsulated ^3He atom, the encapsulated H_2 , H_2O or NH_3 molecule can be employed as a sensitive NMR probe to investigate the ring currents of fullerene cages and to follow chemical reactions of endofullerenes at the exterior of the fullerene cage.

Acknowledgments

The authors are grateful for financial support from the National Natural Science Foundation of China (20572105 and 20621061) and the National Basic Research Program of China (2006CB922003). We also thank the USTC Supercomputer Center for computational resources.

- [1] K. M. Kadish, R. S. Ruoff, *Fullerenes: Chemistry, Physics, and Technology*, Wiley, New York, **2000**, chapters 8 and 9.
- [2] a) K. M. Kadish, R. S. Ruoff, *Fullerenes: Chemistry, Physics, and Technology*, John Wiley & Sons, New York, **2000**, pp. 357–393; b) H. Shinohara, *Rep. Prog. Phys.* **2000**, 63, 843–892.
- [3] a) M. Saunders, H. A. Jiménez-Vázquez, R. J. Cross, S. Mroczkowski, M. L. Cross, D. E. Giblin, R. J. Poreda, *J. Am. Chem. Soc.* **1994**, 116, 2193–2194; b) M. Saunders, H. A. Jiménez-Vázquez, R. J. Cross, S. Mroczkowski, D. I. Freedberg, F. A. L. Anet, *Nature* **1994**, 367, 256–258; c) M. Saunders, R. J. Cross, H. A. Jiménez-Vázquez, R. Shimshi, A. Khong, *Science* **1996**, 271, 1693–1697.
- [4] a) Y. Rubin, T. Jarrosson, G.-W. Wang, M. D. Bartberger, K. N. Houk, G. Schick, M. Saunders, R. J. Cross, *Angew. Chem. Int. Ed.* **2001**, 40, 1543–1546; b) C. M. Stanisky, R. J. Cross, M. Saunders, M. Murata, Y. Murata, K. Komatsu, *J. Am. Chem. Soc.* **2005**, 127, 299–302; c) S.-C. Chuang, Y. Murata, M. Murata, K. Komatsu, *Chem. Commun.* **2007**, 1751–1753.
- [5] a) Y. Murata, M. Murata, K. Komatsu, *J. Am. Chem. Soc.* **2003**, 125, 7152–7153; b) S. Iwamatsu, S. Murata, Y. Andoh, M. Minoura, K. Kobayashi, N. Mizorogi, S. Nagase, *J. Org. Chem.* **2005**, 70, 4820–4825; c) S.-C. Chuang, Y. Murata, M. Murata, S. Mori, S. Maeda, F. Tanabe, K. Komatsu, *Chem. Commun.* **2007**, 1278–1280; d) S.-C. Chuang, Y. Murata, M. Murata, K. Komatsu, *J. Org. Chem.* **2007**, 72, 6447–6453; e) Y. Murata, S. Maeda, M. Murata, K. Komatsu, *J. Am. Chem. Soc.* **2008**, 130, 6702–6703.
- [6] a) K. Komatsu, M. Murata, Y. Murata, *Science* **2005**, 307, 238–240; b) M. Murata, Y. Murata, K. Komatsu, *J. Am. Chem. Soc.* **2006**, 128, 8024–8033.
- [7] a) S. Iwamatsu, T. Uozaki, K. Kobayashi, S. Re, S. Nagase, S. Murata, *J. Am. Chem. Soc.* **2004**, 126, 2668–2669; b) S. Iwamatsu, S. Murata, *Tetrahedron Lett.* **2004**, 45, 6391–6394; c) Z. Xiao, J. Yao, D. Yang, F. Wang, S. Huang, L. Gan, Z. Jia, Z. Jiang, X. Yang, B. Zheng, G. Yuan, S. Zhang, Z. Wang, *J. Am. Chem. Soc.* **2007**, 129, 16149–16162.
- [8] S. Iwamatsu, C. M. Stanisky, R. J. Cross, M. Saunders, N. Mizorogi, S. Nagase, S. Murata, *Angew. Chem. Int. Ed.* **2006**, 45, 5337–5340.
- [9] K. E. Whitener Jr., M. Frunzi, S. Iwamatsu, S. Murata, R. J. Cross, M. Saunders, *J. Am. Chem. Soc.* **2008**, 130, 13996–13999.
- [10] R. C. Haddon, A. Pasquarello, *Phys. Rev. B* **1994**, 50, 16459–16463.
- [11] a) J. Cioslowski, *J. Am. Chem. Soc.* **1994**, 116, 3619–3620; b) M. Bühl, W. Thiel, H. Jiao, P. v. R. Schleyer, M. Saunders, F. A. L. Anet, *J. Am. Chem. Soc.* **1994**, 116, 6005–6006; c) J. Cioslowski, *Chem. Phys. Lett.* **1994**, 227, 361–364; d) M. Bühl, W. Thiel, *Chem. Phys. Lett.* **1995**, 233, 585–589; e) M. Bühl, W. Thiel, U. Schneider, *J. Am. Chem. Soc.* **1995**, 117, 4623–4627; f) M. Bühl, C. v. Wüllen, *Chem. Phys. Lett.* **1995**, 247, 63–68; g) M. Bühl, S. Patchkovskii, W. Thiel, *Chem. Phys. Lett.* **1997**, 275, 14–18; h) M. Bühl, *Chem. Eur. J.* **1998**, 4, 734–739; i) M. Bühl, M. Kaupp, O. L. Malkina, V. G. Malkin, *J. Comput. Chem.* **1999**, 20, 91–105; j) Z. Chen, J. Cioslowski, N. Rao, D. Monsieff, M. Bühl, A. Hirsch, W. Thiel, *Theor. Chem. Acc.* **2001**, 106, 364–368; k) M. Bühl, A. Hirsch, *Chem. Rev.* **2001**, 101, 1153–1183.
- [12] G.-W. Wang, X.-H. Zhang, H. Zhan, Q.-X. Guo, Y.-D. Wu, *J. Org. Chem.* **2003**, 68, 6732–6738.
- [13] a) Z.-X. Chen, G.-W. Wang, *J. Org. Chem.* **2005**, 70, 2380–2383; b) G.-W. Wang, J.-X. Li, Y.-J. Li, Y.-C. Liu, *J. Org. Chem.* **2006**, 71, 680–684; c) G.-W. Wang, F.-B. Li, T.-H. Zhang, *Org. Lett.* **2006**, 8, 1355–1358; d) G.-W. Wang, X.-P. Chen, X. Cheng, *Chem. Eur. J.* **2006**, 12, 7246–7253; e) G.-W. Wang, F.-B. Li, Y. Xu, *J. Org. Chem.* **2007**, 72, 4774–4778; f) G.-W. Wang, F.-B. Li, Z.-X. Chen, B. Chen, Y. Xu, *J. Org. Chem.* **2007**, 72, 4479–4483; g) F.-B. Li, T.-X. Liu, G.-W. Wang, *J. Org. Chem.* **2008**, 73, 6417–6420.
- [14] M. J. S. Dewar, E. G. Zoebisch, E. F. Healy, J. J. P. Stewart, *J. Am. Chem. Soc.* **1985**, 107, 3902–3909.
- [15] J. J. P. Stewart, *J. Comput. Chem.* **1989**, 10, 210–264.
- [16] K. Wolinski, J. F. Hinton, P. Pulay, *J. Am. Chem. Soc.* **1990**, 112, 8251–8260.
- [17] A. D. Becke, *J. Chem. Phys.* **1993**, 98, 5648–5652.
- [18] C. Lee, W. Yang, R. G. Parr, *Phys. Rev. B* **1988**, 37, 785–789.
- [19] The terminology of “scaled chemical shifts” may also be used here.
- [20] M. J. Frisch, G. W. Trucks, H. B. Schlegel, G. E. Scuseria, M. A. Robb, J. R. Cheeseman, J. A. Montgomery Jr, T. Vreven, K. N. Kudin, J. C. Burant, J. M. Millam, S. S. Iyengar, J. Tomasi, V. Barone, B. Mennucci, M. Cossi, G. Scalmani, N. Rega,

- G. A. Petersson, H. Nakatsuji, M. Hada, M. Ehara, K. Toyota, R. Fukuda, J. Hasegawa, M. Ishida, T. Nakajima, Y. Honda, O. Kitao, H. Nakai, M. Klene, X. Li, J. E. Knox, H. P. Hratchian, J. B. Cross, C. Adamo, J. Jaramillo, R. Gomperts, R. E. Stratmann, O. Yazyev, A. J. Austin, R. Cammi, C. Pomelli, J. W. Ochterski, P. Y. Ayala, K. Morokuma, G. A. Voth, P. Salvador, J. J. Dannenberg, V. G. Zakrzewski, S. Dapprich, A. D. Daniels, M. C. Strain, O. Farkas, D. K. Malick, A. D. Rabuck, K. Raghavachari, J. B. Foresman, J. V. Ortiz, Q. Cui, A. G. Baboul, S. Clifford, J. Cioslowski, B. B. Stefanov, G. Liu, A. Liashenko, P. Piskorz, I. Komaromi, R. L. Martin, D. J. Fox, T. Keith, M. A. Al-Laham, C. Y. Peng, A. Nanayakkara, M. Challacombe, P. M. W. Gill, B. Johnson, W. Chen, M. W. Wong, C. Gonzalez, J. A. Pople, *Gaussian 03, Revision B.03*, Gaussian, Inc., Pittsburgh, PA, **2003**.
- [21] a) M. Matsuo, H. Isobe, T. Tanaka, Y. Murata, M. Murata, K. Komatsu, E. Nakamura, *J. Am. Chem. Soc.* **2005**, *127*, 17148–17149.
- [22] a) M. Saunders, H. A. Jiménez-Vázquez, B. W. Bangerter, R. J. Cross, S. Mroczkowski, D. I. Freedberg, F. A. L. Anet, *J. Am. Chem. Soc.* **1994**, *116*, 3621–3622; b) A. B. Smith III, R. M. Strongin, L. Brard, W. J. Romanow, M. Saunders, H. A. Jiménez-Vázquez, R. J. Cross, *J. Am. Chem. Soc.* **1994**, *116*, 10831–10832; c) R. J. Cross, H. A. Jiménez-Vázquez, Q. Lu, M. Saunders, D. I. Schuster, S. R. Wilson, H. Zhao, *J. Am. Chem. Soc.* **1996**, *118*, 11454–11459; d) G.-W. Wang, B. R. Weedon, M. S. Meier, M. Saunders, R. J. Cross, *Org. Lett.* **2000**, *2*, 2241–2243; e) G.-W. Wang, M. Saunders, R. J. Cross, *J. Am. Chem. Soc.* **2001**, *123*, 256–259.
- [23] G. Otero, G. Biddau, C. Sánchez-Sánchez, R. Caillard, M. F. López, C. Rogero, F. J. Palomares, N. Cabello, M. A. Basanta, J. Ortega, J. Méndez, A. M. Echavarren, R. Pérez, B. Gómez-Lor, J. A. Martín-Gago, *Nature* **2008**, *454*, 865–868.
- [24] K. Komatsu, G.-W. Wang, Y. Murata, T. Tanaka, K. Fujiwara, *J. Org. Chem.* **1998**, *63*, 9358–9366.

Received: October 23, 2008

Published Online: January 13, 2009